Supplemental Information

Instrument-free synthesizable fabrication of label-free optical biosensing paper strips for the early detection of infectious keratoconjunctivitides

Wansun Kim, Jae-Chul Lee, Jae-Ho Shin, Kyung-Hyun Jin, Hun-Kuk Park*, Samjin Choi*

Department of Biomedical Engineering,
College of Medicine,
Kyung Hee University,
Seoul 130-701,
South Korea

***Address for correspondence:**
Samjin Choi, Ph.D., and Hun-Kuk Park, M.D., Ph.D.,
Department of Biomedical Engineering,
College of Medicine,
Kyung Hee University,
1 Hoegi-dong,
Dongdaemun-gu,
Seoul 130-701,
South Korea
Tel: +82 2 961 0290
Fax: +82 2 6008 5535
E-mail: medchoi@khu.ac.kr

■ Raman spectrum of 2-NAT molecule

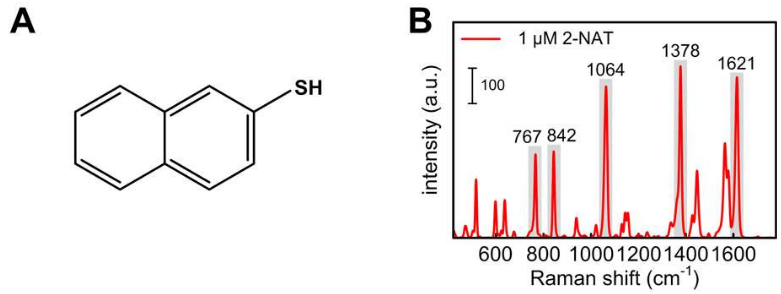

Figure S1. (A) The molecular structure of 2-naphthalenethiol (2-NAT) and (B) Raman spectra of a 1 μM 2-NAT molecule for GNPs deposited on paper with optimal SILAR condition. The prominent Raman peaks of the 2-NAT molecule were obtained at 767 cm^{-1} (C−H wag), 842 cm^{-1} (C−H twist), 1064 cm^{-1} (symmetric C−H bend), 1378 cm^{-1} (ring stretch), and 1621 cm^{-1} (ring stretch).

■ Distribution of GNPs with number of SILAR cycles (10 mM SILAR reagents)

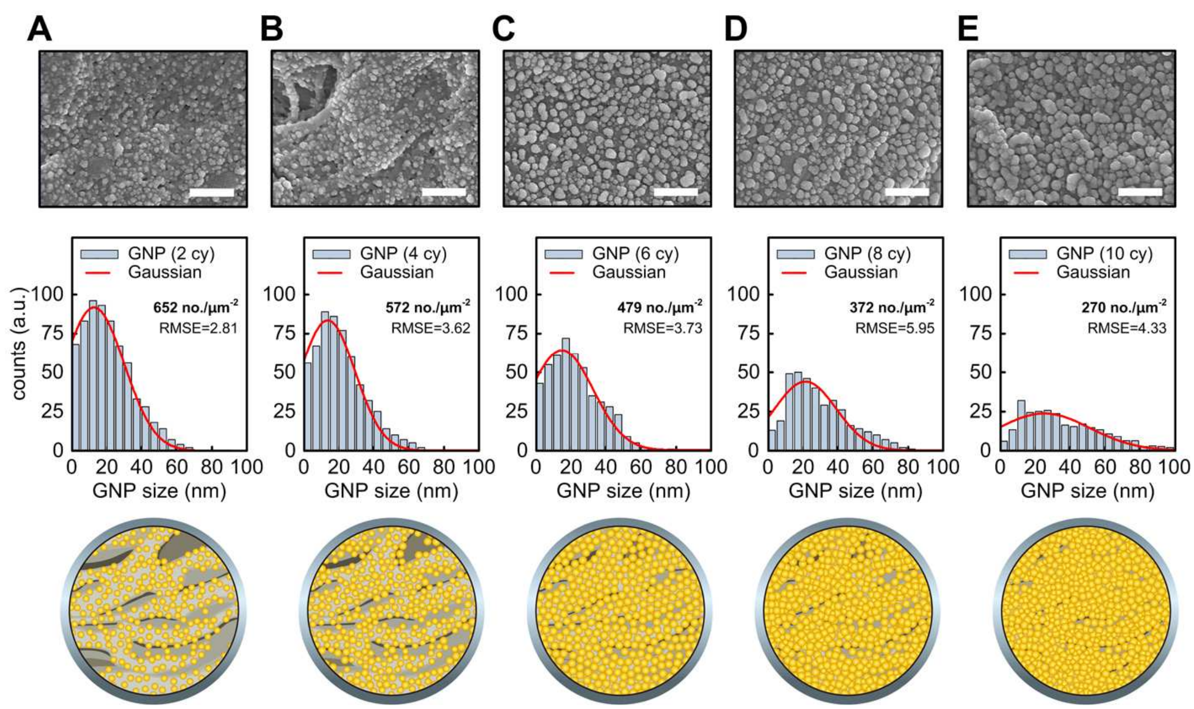

Figure S2. Distributions of SILAR-synthesized GNPs deposited on paper with (A) two, (B) four, (C) six, (D) eight, and (E) 10 SILAR cycles (top: SEM. Scale bar=250 nm; middle: GNP distribution; bottom: schematic distribution). The surface density of GNP was represented by the number of GNP per unit area (no./μm^{-2}). RMSE indicates the root mean square error between the Gaussian-predicted data and experimental data.

■ Distribution of SILAR reagent-concentrated GNPs with number of SILAR cycles

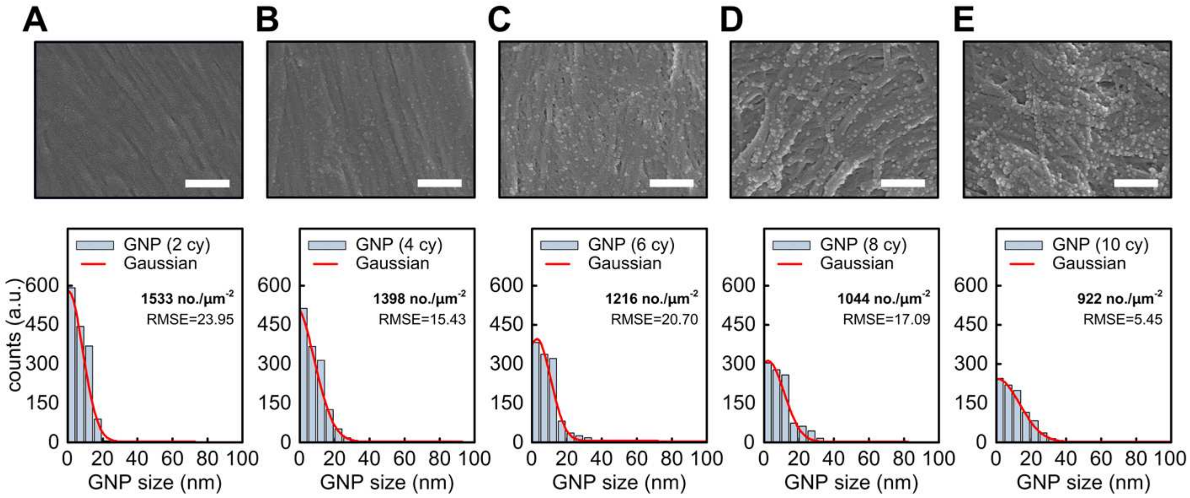

Figure S3. Distributions of SILAR-synthesized GNPs deposited on paper with (A) two, (B) four, (C) six, (D) eight, and (E) 10 SILAR using 1 mM $HAuCl_4$ and $NaBH_4$ SILAR reagents. (top: SEM. Scale bar=250 nm; bottom: GNP distribution). The surface density of GNP was represented by the number of GNP per unit area (no./μm^{-2}). RMSE indicates the root mean square error between the Gaussian-predicted data and experimental data.

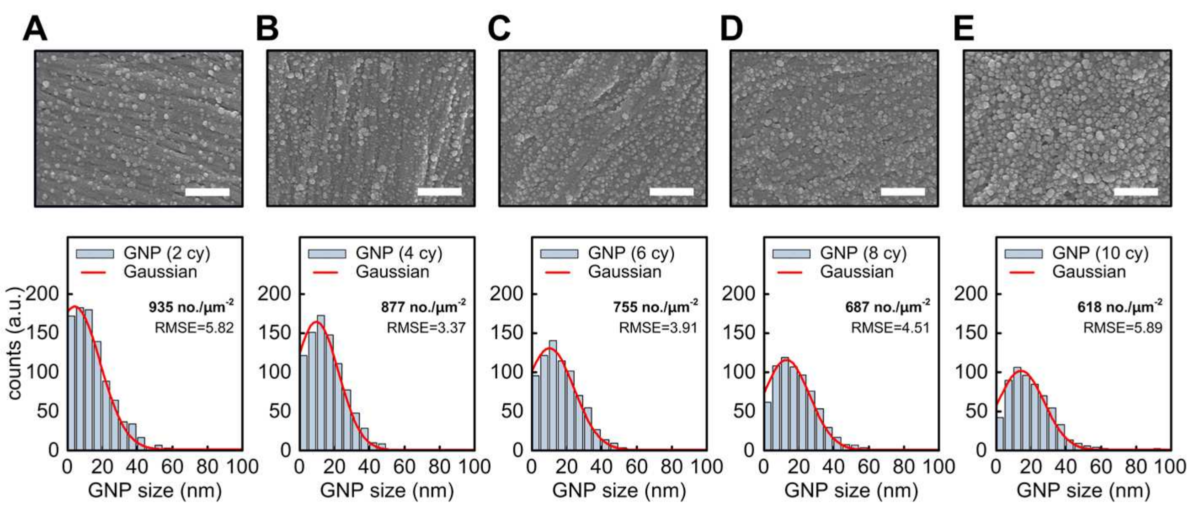

Figure S4. Distributions of SILAR-synthesized GNPs deposited on paper with (A) two, (B) four, (C) six, (D) eight, and (E) 10 SILAR using 5 mM $HAuCl_4$ and $NaBH_4$ SILAR reagents. (top: SEM. Scale bar=250 nm; bottom: GNP distribution). The surface density of GNP was represented by the number of GNP per unit area (no./μm^{-2}). RMSE indicates the root mean square error between the Gaussian-predicted data and experimental data.

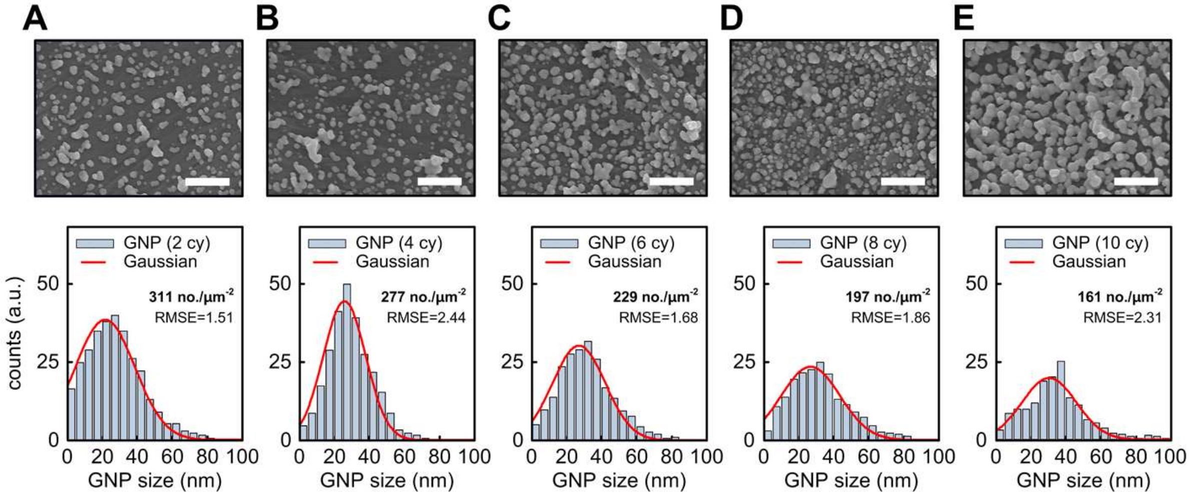

Figure S5. Distributions of SILAR-synthesized GNPs deposited on paper with (A) two, (B) four, (C) six, (D) eight, and (E) 10 SILAR using 20 mM SILAR $HAuCl_4$ and $NaBH_4$ reagents. (top: SEM. Scale bar=250 nm; bottom: GNP distribution). The surface density of GNP was represented by the number of GNP per unit area (no./μm^{-2}). RMSE indicates the root mean square error between the Gaussian-predicted data and experimental data.

■ Computational modeling

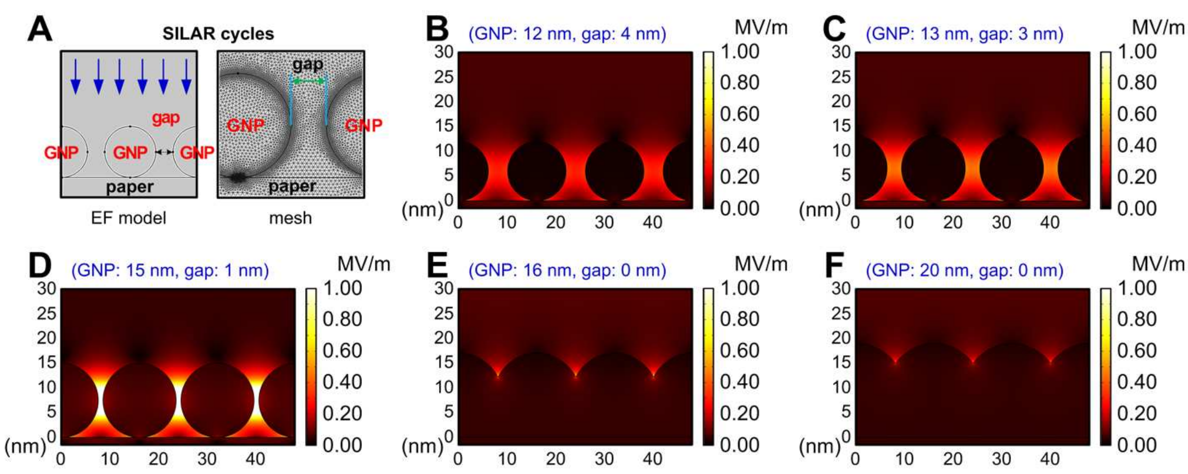

Figure S6. (A) Finite element model of GNPs with SILAR cycles and computational results of GNP diameter and interparticle gap distance-dependent LSPR effect with (B) two, (C) four, (D) six, (E) eight, and (F) 10 SILAR cycles on the electromagnetic field (EF).

■ Sensitivity

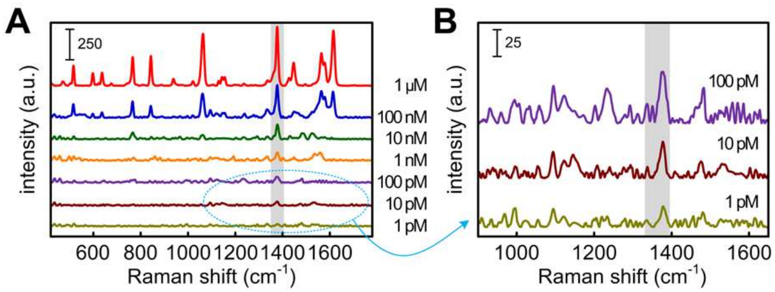

Figure S7. Representative SERS spectra with (A) different 2-NAT concentrations (10^{-12} ~10^{-6} M) and (B) low concentrations of 2-NAT on SILAR-synthesized GNPs deposited on SERS paper. Gray indicates a 2-NAT molecule-characterized peak at 1378 cm^{-1}.

■ Enhancement factor

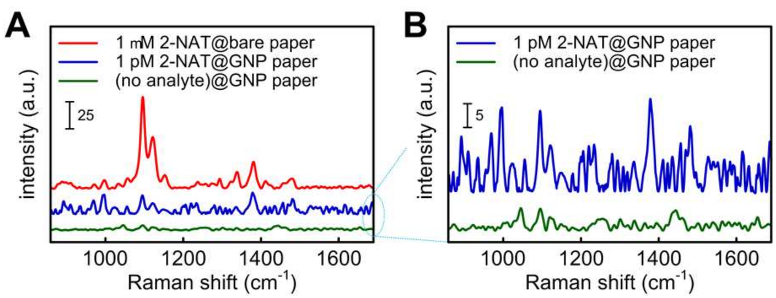

Figure S8. Raman spectra of 1 mM 2-NAT on bare paper and 1 pM 2-NAT and no analyte on SILAR-synthesized GNP paper strip.

The enhancement factor (EF) was calculated as the difference in Raman intensity between two different substrates as

$$EF = \left(\frac{I_{SERS}}{I_{bare}}\right)\left(\frac{N_{bare}}{N_{SERS}}\right), \tag{S1}$$

where I_{SERS} and I_{bare} are the Raman intensity of the molecule on the SERS and bare papers, respectively, and N_{SERS} and N_{bare} are the average number of adsorbed molecules in the scattering volume for SERS and non-SERS areas, respectively.[1] Assuming that the probe molecules were uniformly distributed on the substrates, the number of adsorbed molecules can be estimated as

$$N = \left(N_A \cdot c \cdot \frac{V_{droplet}}{A_{spot}}\right) A_{laser}, \tag{S2}$$

where N_A is Avogadro's constant, c is the concentration of the probe molecule, V is the volume of the molecule droplet, A_{spot} is the size of the substrate, and A_{laser} is the size of the laser spot.[2] Since the same methods for assessing the Raman measurement were applied to two substrates, the parameters of N_A for 2-NAT, V, A_{spot}, and A_{laser} were the same.

Therefore, Eq. (S2) can be written as

$$EF = \left(\frac{I_{SERS}}{I_{bare}}\right)\left(\frac{c_{bare}}{c_{SERS}}\right), \tag{S3}$$

where c_{SERS} and c_{R} are the concentration of 2-NAT molecule on the GNP and bare papers, respectively.

■ Bio-applications

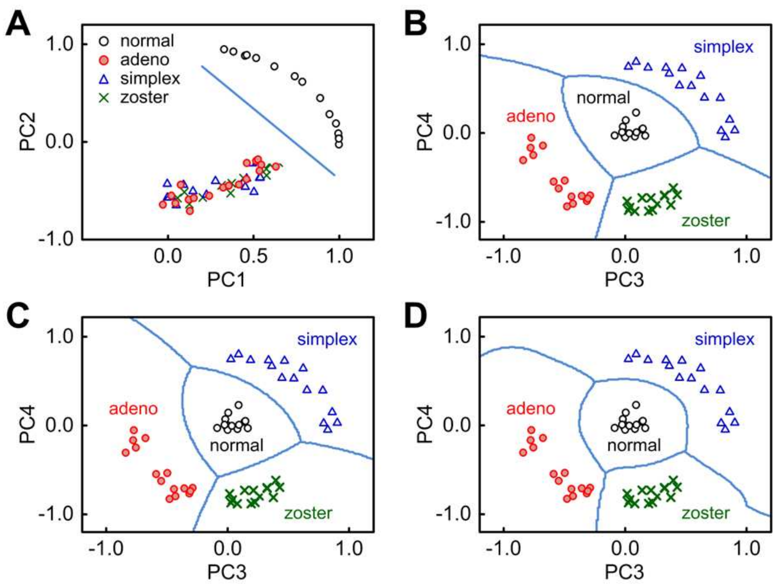

Figure S9. PCA-SVM scores (n=15, each): (A) to detect the presence of keratoconjunctivitis using SVM classifier with linear kernel and to classify the normal eye and keratoconjunctivitides using SVM classifier with (B) the second-order polynomial kernel (*d*=2, Eq. S4), (C) Gaussian kernel (*σ*=2, Eq. S5), and (D) Hilbert transform radial basis function kernel (*ρ*=2, *a*=1, *b*=2, Eq. S6).[3,4]

$$K_{poly}\left(\mathbf{x}_1,\mathbf{x}_2\right) = \left(\left\langle \mathbf{x}_1 \cdot \mathbf{x}_2 \right\rangle + 1\right)^d \tag{S4}$$

$$K_{Gaussian}\left(\mathbf{x}_1,\mathbf{x}_2\right) = \exp\left(-\left\|\mathbf{x}_1 - \mathbf{x}_2\right\|^2 \big/ 2\sigma^2\right) \tag{S5}$$

$$K_{HtBRF}\left(\mathbf{x}_1,\mathbf{x}_2\right) = \exp\left(-\rho \sum\nolimits_i \left|\mathbf{x}_{1i}^{\,a} - \mathbf{x}_{2i}^{\,a}\right|^b\right) \tag{S6}$$

■ References

(1) Le Ru, E. C.; Blackie, E.; Meyer, M.; Etchegoin, P. G. *J. Phys. Chem. C* **2007**, *111* (37), 13794–13803.

(2) Liu, X.; Shao, Y.; Tang, Y.; Yao, K.-F. *Sci. Rep.* **2014**, *4*, 5835.

(3) Choi, S.; Jiang, Z. *Comput. Biol. Med.* **2010**, *40* (1), 8–20.

(4) Jung, G. B.; Nam, S. W.; Choi, S.; Lee, G.-J.; Park, H.-K. *Biomed. Opt. Express* **2014**, *5* (9), 3238.